Nano Research
2023, 16(11): 12821–12829

ISSN 1998-0124 CN 11-5974/O4
https://doi.org/10.1007/s12274-023-6209-6

Research Article

Enhanced composite thermal conductivity by percolated networks of *in-situ* confined-grown carbon nanotubes

Xiao Zhang[1,2] (✉), Wei Tan[2,†], Tian Carey[3,‡], Bo Wen[2,3,⊥], Delong He[4], Adrees Arbab[3], Alex Groombridge[2,5], Fiona Smail[2], Jean de La Verpilliere[2,5], Chengning Yao[6], Yanchun Wang[1], Xiaojun Wei[1], Huaping Liu[1], Sishen Xie[1], Felice Torrisi[3,6,7], Michael De Volder[2] (✉), Weiya Zhou[1] (✉), and Adam Boies[2] (✉)

[1] *Beijing National Laboratory for Condensed Matter Physics, Institute of Physics, Chinese Academy of Sciences, Beijing 100190, China*
[2] *Department of Engineering, University of Cambridge, Cambridge CB2 1PZ, UK*
[3] *Cambridge Graphene Centre, Engineering Department, University of Cambridge, Cambridge CB3 0FA, UK*
[4] *Université Paris-Saclay, Centrale-Supélec, ENS Paris-Saclay, CNRS, LMPS-Laboratoire de Mécanique Paris-Saclay, 91190, Gif-sur-Yvette, France*
[5] *Echion Technologies, Cambridge CB22 3FG, UK*
[6] *Molecular Sciences Research Hub, Imperial College London, London W12 0BZ, UK*
[7] *Dipartimento di Fisica e Astronomia, Universita' di Catania, Catania 64 95123, Italy*
[†] *Present address: School of Engineering and Materials Science, Queen Mary University of London, London E1 4NS, UK*
[‡] *Present address: School of Physics, CRANN & AMBER Research Centres, Trinity College Dublin, Dublin D02 E8C0, Ireland*
[⊥] *Present address: Jaguar Land Rover, Banbury Road Gaydon, Lighthorne Heath, Warwick CV35 0RR, UK*

Received: 19 July 2023 / **Revised:** 8 September 2023 / **Accepted:** 17 September 2023

ABSTRACT

Despite the ever-increasing demand of nanofillers for thermal enhancement of polymer composites with higher thermal conductivity and irregular geometry, nanomaterials like carbon nanotubes (CNTs) have been constrained by the nonuniform dispersion and difficulty in constructing effective three-dimensional (3D) conduction network with low loading and desired isotropic or anisotropic (specific preferred heat conduction) performances. Herein, we illustrated the *in-situ* construction of CNT based 3D heat conduction networks with different directional performances. First, to *in-situ* construct an isotropic percolated conduction network, with spherical cores as support materials, we developed a confined-growth technique for CNT-core sea urchin (CNTSU) materials. With 21.0 wt.% CNTSU loading, the thermal conductivity of composites reached 1.43 ± 0.13 W/(m·K). Secondly, with aligned hexagonal boron nitride (hBN) as an anisotropic support, we constructed CNT-hBN aligned networks by *in-situ* CNT growth, which improved the utilization efficiency of high density hBN and reduced the thermal interface resistance between matrix and fillers. With ~ 8.5 wt.% loading, the composites possess thermal conductivity up to 0.86 ± 0.14 W/(m·K), 374% of that for neat matrix. Due to the uniformity of CNTs in hBN network, the synergistic thermal enhancement from one-dimensional (1D) + two-dimensional (2D) hybrid materials becomes more distinct. Based on the detailed experimental evidence, the importance of purposeful production of a uniformly interconnected heat conduction 3D network with desired directional performance can be observed, particularly compared with the traditional direct-mixing method. This study opens new possibilities for the preparation of high-power-density electronics packaging and interfacial materials when both directional thermal performance and complex composite geometry are simultaneously required.

KEYWORDS

carbon nanotubes, hexagonal boron nitride, thermal conductivity, composites, three-dimensional printing

1 Introduction

With the rapid progress of computer-assisted driving, battery management, and 5G technology, heat dissipation from high-power-density electronics and associated packaging or interfacial materials have become increasingly critical in guaranteeing electronics performance and reliability [1–4]. The heat dissipation components need to be easily manufactured, highly thermally conductive, lightweight, and geometry adaptive [2]. For these purposes, commonly used polymer materials have been enhanced by mixing with micro or nano fillers with high thermal conductivity (κ), such as carbon nanoparticles [5–11], boron nitride [12–17], and other ceramic particles [4], particularly by direct-mixing, to improve the thermal conductivity of resulting composites (κ_{CP}). Among these fillers, carbon nanotubes (CNTs) have attracted special attention due to the intrinsic high thermal conductivity (κ ~ 3000 W/(m·K)) and high aspect ratio, thus facilitating formation of efficient heat conduction pathway within polymer matrix [18]. However, commonly only a modest κ_{CP} increase had been obtained, mostly because of filler being isolated and randomly distributed at low loading during the process of being mixed with polymer and curing. These methods result in a

Address correspondence to Xiao Zhang, zhangx@iphy.ac.cn; Michael De Volder, mfld2@cam.ac.uk; Weiya Zhou, wyzhou@iphy.ac.cn; Adam Boies, amb233@cam.ac.uk

poorly conductive polymer (κ = 0.1–0.2 W/(m·K)) due to a lack of a percolated network, as well as the contact resistance between the fillers and the high interfacial thermal resistance between fillers and surrounding polymer matrix [19]. Nevertheless, higher CNT loading significantly increases the processing challenge due to the dramatically increased viscosity and fillers agglomeration. Therefore, to effectively increase κ_{CP}, a preset three-dimensional (3D) interconnected CNT network uniformly distributed within the composite is essential, which also needs to survive the compounding process and occupy increased fraction in a matrix [18].

In our previous research, with *in-situ* polymerization, CNT sheets fabricated by stacking ~ 10^3 CNT films produced by continuous chemical vapor deposition (CVD) were used as the filler [20]. The preset heat conduction network from CNT sheet endows composites with high κ_{CP}, but the enhancements are isolated to the in-plane direction due to the highly anisotropic conductivity of multi-layered CNT sheet (in-plane κ ~ 120 W/(m·K) and the normal direction κ ~ 0.1 W/(m·K)). Moreover, CNT vertical arrays (CNT forests) have been extensively explored as thermal interface materials, which can achieve high κ_{CP} solely in normal direction of sheet composites because of the alignment of CNTs passing through the whole thickness, but their geometries are still limited by the array dimension scale [8, 21]. Thus, constructing 3D interconnected CNT percolated networks simultaneously with geometric flexibility and designed directional thermal performance (isotropic or preferred directional) is critically important for the complex thermal application of enhanced composites.

Herein, we developed a method for *in-situ* CNT growth and polymer infiltration on optimized support to design the efficient isotropic or anisotropic heat conduction pathway. We adopted spherical cores and hexagonal boron nitride (hBN) two-dimensional (2D) materials as support materials to preset CNT-based isotropic and anisotropic three-dimensional (3D) interconnected networks, respectively. With spherical cores as support, the hybrid CNT-cores sea urchin (CNTSU) structure has been synthesized within a confined space to form a highly interconnected bulk material, with which high and uniform filler loading can be realized in synthesis of enhanced isotopically thermal conductive composites. Additionally, with hBN as support, an aligned CNT-hBN network was *in-situ* grown with uniform hybrid distribution and used in constructing the anisotropic thermal conduction composites. To address challenges with the relative high density and low aspect ratio for hBN powder, we developed a directional ice-templating self-assembly method. The utilization efficiency of hBN and uniformity of hybrid fillers have been improved with lower filler loading (< 10 wt.%). The one-dimensional (1D) + 2D synergistic effects [5, 22, 23] from CNT-hBN hybrid nanomaterials are discussed.

2 Experimental details

2.1 Confined-growth of hybrid CNT-cores (CNT sea urchin) highly interconnected isotropic networks

The cores to grow CNTSU were continuously synthesized by our previous reported spray-drying method [24]. Briefly, aqueous solution of aluminum nitrate and iron nitrate was atomized with nitrogen carrier gas to form micron droplets aerosol which then in-line dried and calcinated to produce a high concentration of micron hollow cores with iron islands randomly distributed among alumina.

Following our previous report, the CNTSU can be continuously grown in-line (referred as continuous-growth) [24] and freely grown *ex-situ* on the substrate (referred as free-growth). However, to achieve high CNT density and closely interconnected CNTSU fillers, we developed a confined-growth method to densify the expanding CNTSUs during growth and fill the mold (Fig. 1(a)).

A critical requirement of the confined-growth was the porous and demountable growth cage (Figs. 1(b) and 1(d), and Fig. S1 in the Electronic Supplementary Material (ESM)) which was 3D printed with the Form2 SLA 3D Printer equipped with the ceramic resin (SiO_2 particle included). After being trimmed and fired, all the growth cage components transformed into silica ceramic texture which can tolerate the high CNT growth temperature and reaction gases.

Mixed with isopropyl alcohol (IPA) to form slurry, cores were coated onto anodic aluminum oxide (AAO, Whatman Anodisc 47, 60 μm thick with 200 nm nominal pore size through-holes) substrate. After covered by another piece of AAO, this AAO-cores-AAO sandwich was assembled with the growth cage, and inserted into the CVD growth furnace set to 800 °C (Figs. 1(c) and 1(d)). With helium as the carrier gas, the cores were firstly reduced by hydrogen for 10 min. After the flow of ethylene (mixed carbon source), the CNT growth lasted for ~ 1 h, and then reaction gases were flushed by pure helium before furnace was cooled down. The resulting CNTSU bulk material was strong enough to be free-standing and released from cage and AAO substrates (Figs. 1(e) and 1(f)). The thickness of final CNTSU bulk materials can be tuned from 1 to 3 mm by changing the thickness of ceramic covering weight & occupier and the slurry thickness.

2.2 Preparation of aligned hBN support and *in-situ* construction of hybrid CNT-hBN networks

The hBN nanoflakes (hBNNFs) were produced by exfoliating hBN powders (Goodfellows B516011) within a shear fluid processor (microfluidizer, M-110P, Microfluidics International Corporation, Westwood, MA, USA) [25]. Carboxymethylcellulose sodium salt (CMC, average molecular weight = 700,000, Aldrich No. 419338) was added to stabilize the hBN in solution. The hBN solution came as an aqueous ink with hBNNFs concentration of 0.44 mg/mL. The hBNNFs' lateral size was ~ 520 nm, and thickness followed a log-normal distribution peaking at 9 nm.

As shown in Fig. 2, a steel mold containing the inks with desired filler concentration was placed onto a large heat sink which was cooled in advance to liquid nitrogen temperature. With a fast anisotropic freeze casting process, hBNNFs were expelled out from layered ice crystal [26], forming a well aligned network vertically along the temperature gradient. After freeze-drying (Telstar® LyoQuest Freeze Dryer) for 48 h, the aligned support network (aerogel) of pure hBN can be obtained.

The hybrid CNT-hBN network was produced by firstly mixing the hBNNFs ink with Fe_2O_3 nanopowder (~ 5 nm, Alfa Aesar 044296.09) and then followed the same process to prepare the red Fe_2O_3 NP-hBN network which was used for a standard CNT growth (similar to CNTSU). The *in-situ* grown CNT outstretched from the hBNNFs, formed the final hybrid CNT-hBN network.

2.3 Preparation of thermal enhanced composites by *in-situ* polymerization

Both above hybrid networks were impregnated through the *in-situ* polymerization of epoxy which was firstly diluted with acetone and followed by evaporation of the acetone under vacuum, and by curing with a vacuum bag method as sketched in Fig. 3. The epoxy resin was bisphenol-A IN2 infusion resin and a hexane hardener (Easy Composites Ltd). The epoxy resin and hardener were mixed in the proportion 10:3 by mass. By repeating the infiltration process before curing, the voids inside network can be

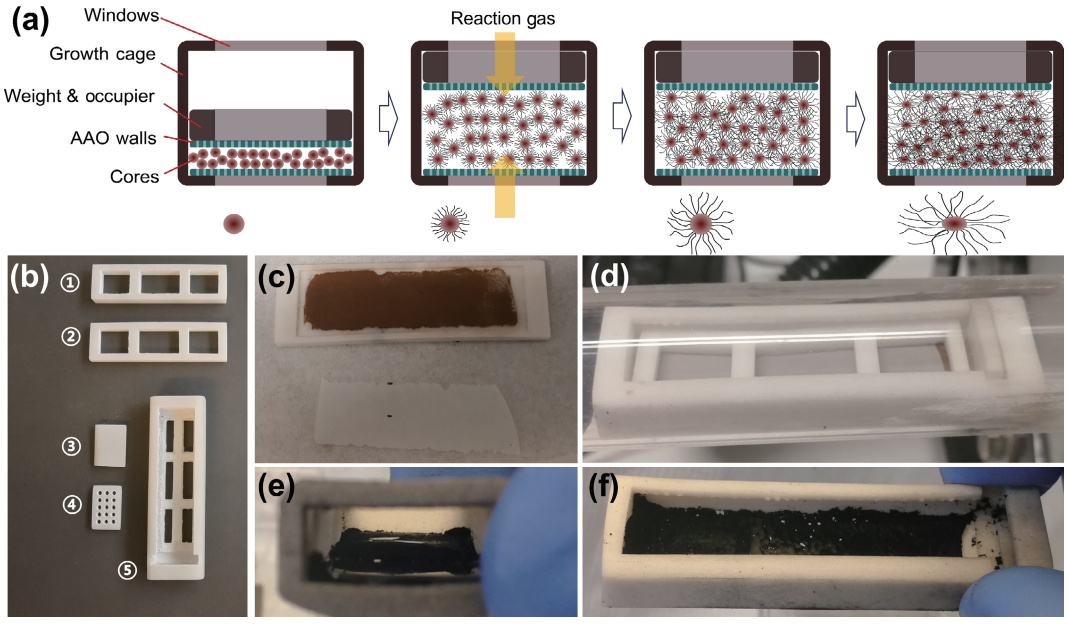

Figure 1 Confined-growth of CNTSU with a 3D printed growth cage. (a) Schematic diagram of the CG-CNTSU and the morphology evolution of individual CNTSU. (b) After being trimmed and fired, the polymer matrix within component precursors burned away, leaving the model transformed into a silica ceramic texture which can tolerate 1100 °C. Within these components, ① and ② are the cover weight & occupier with different thickness to tune the thicknesses of grown bulk materials; ③ and ④ are the mountable side walls facilitating cores loading and CNTSU unloading; ⑤ is the main body of the cage. ((c) and (d)) After the cores were blade-coated onto the bottom AAO, they were successively constrained by the covering AAO, assembled with other cage components, and inserted into quartz tube for CVD growth. ((e) and (f)) After standard CNT growth process, the CG-CNTSU bulk materials were synthesized with desired thickness.

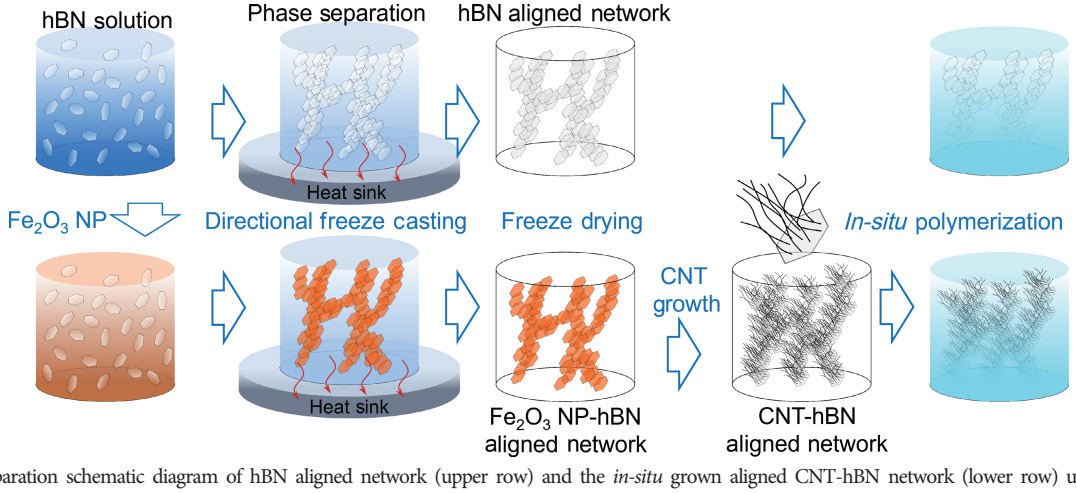

Figure 2 Preparation schematic diagram of hBN aligned network (upper row) and the *in-situ* grown aligned CNT-hBN network (lower row) used as thermal enhancement hybrid fillers.

effectively filled, benefiting from the capillary force and vacuum environment. The impregnated hybrid networks were located within a polytetrafluoroethylene (PTFE) mold to tune the nominal thickness of 1–2 mm. An outer breather layer cloth and a vacuum bagging system (Easy Composites Ltd) were incorporated to apply a consolidation pressure of P = 0.1 MPa (one atmosphere), at a temperature of 40 °C for 1 h. Excess resin was absorbed by the breather layer cloth during consolidation. Samples were then cured at 120 °C for 3 h, with a constant pressure of 0.1 MPa to guarantee full polymerization. For the resulting composites, both CNTs and the attached substrates (cores or hBN) were counted as the filler weight when calculating the weight percentage.

As control groups, CNTSU powders, hBN powders, and hBN & CNT (NC7000, Nanocyl) hybrid powders were also used as enhancement fillers by direct-mixing. An epoxy resin with uniformly dispersed fillers was obtained by using a planetary mixer (MSK-PCV-300-LD) at 1500 r/min at room temperature for 10 min. The mixture was then degassed in the vacuum oven (ACROSS INTERNATIONAL Elite series) for 1 h and then cured. Polypropylene (PP, Borealis, Belgium)/CNTSU composites were also manufactured using a twin-screw micro extruder (DSM Explore 5 cc Micro Compounder, DSM) for mixing 20 min at 210 °C with the speed of 60 rpm. The composite samples were fabricated via the extrusion-injection method (Micro 5 cc Injection Molder, DSM, Xplore Instruments). The temperatures of the injection nozzle and mould holder were set at 210 and 55 °C, respectively. κ of PP was measured to be 0.22 ± 0.1 W/(m·K), nearly the same as the measured value of epoxy matrix used.

2.4 Characterizations

κ_{CP} was measured according to the ASTM D5470-17 standard using a custom-made steady-state measurement setup (Fig. S2(a) in the ESM) based on the Bi-substrate technique [20]. Square specimens with sides of 10 mm were placed between hot and cold copper blocks which were used as heat flux meters. According to Eq. (1), κ of specimen through thickness at ~37 °C and R_i between specimen and heat flux meters can be directly deduced by linear fitting data obtained from samples with different thicknesses (Δz)

$$\Delta T/q = \Delta z/\kappa + 2/R_i \quad (1)$$

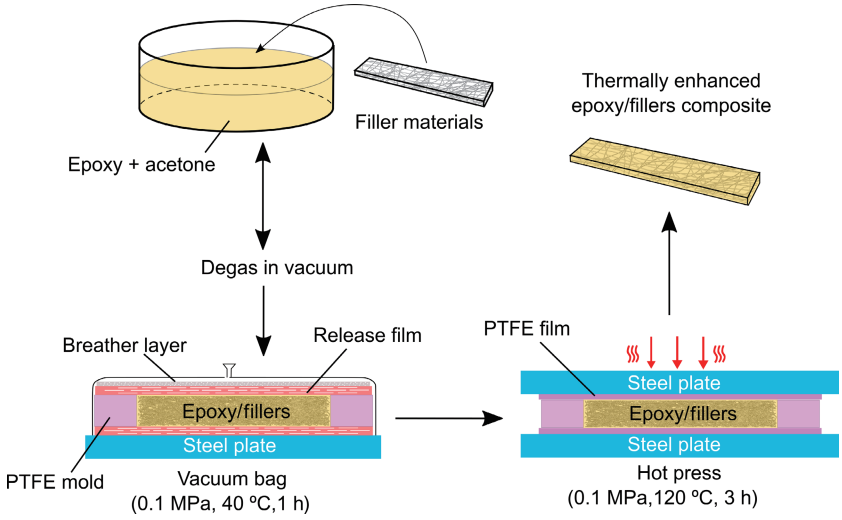

Figure 3 *In-situ* polymerization methodology of epoxy/filler composite manufactured with vacuum bag and hot press methods.

where ΔT was the total temperature drop and q was the heat flux through the sample. Considering the practical engineering application demand, referential errors were calculated by the stochastic error propagation method, generating confidence limits for each calculated κ value. Briefly, during every round of calculation iteration, κ was deduced with a new set of random parameters which were generated based on geometric and thermal parameters' expected values, experimental random/systematic errors, and distribution style.

The scanning electron microscopy (SEM) images were conducted on a field-emission SEM (TESCAN MIRA3). The fracture surfaces of composites were prepared by being cryo-fractured in liquid nitrogen and sputter-coated with a thin layer of gold in a vacuum chamber before SEM observation. Thermogravimetric analysis was conducted with the PerkinElmer Pyris 1 TGA in flowing air environment at 10 K/min heating rate.

3 Results and discussion

3.1 Composites thermally enhanced by hybrid CNT-cores structure (CNTSU)

3.1.1 CNTSU morphology and its thermal enhancing performance by direct-mixing

By using a continuous aerosol process, the alloy micron cores of alumina and iron oxides can be produced at industrial-scale (Fig. 4(a)). The size range of these hollow cores is 0.2–5 μm (mostly 1–2 μm). Because these cores are hollow with shell thickness of several nanometers [24], they can be easily crushed into debris under pressure. With 20 min of free-growth without any space confinement, CNTs were radially grown from embedded iron crystallites on cores to form the hybrid CNTSU structure. The diameter of CNTSUs grown for 20 min is 4–10 μm (Fig. 4(b)) compared with 1–2 μm cores used. With free-growth method, CNTSUs powders were prepared with loose interconnection by the outstretching and entangled CNTs. Details on the resulting CNT structure can be found in our previous study [24].

Compared with other reported CNTSU structures [27], the CNT percentage for our CNTSU is much higher due to dense distributed catalysts sites instead of only decorating tiny amount of catalysts on the cores surface. For the instant in-line CNTSU growth (continuous-growth), the CNT weight percentage is ~ 40 wt.% [24]. By increasing the growth time, larger CNTSUs with more surrounding CNTs were grown (Fig. S3 in the ESM). With 0.3, 1, and 4 h of free-growth, the CNT weight percentage increase to ~ 73.8 wt.%, ~ 91.2 wt.%, and ~ 94.3 wt.%, respectively, based on the thermo gravimetric analysis (TGA) results. However, as the growth time increased to 4 h, grown CNTs tended to curl into wisps instead of continuing expanding and outstretching.

As control groups, we firstly direct-mixed CNTSU within matrix to thermally enhance composites, because CNTSU powders with a lower density of CNTs and higher cores percentage were reported to owe remarkably low thermal percolation threshold (~ 0.15 wt.%) by direct-mixing method [27]. By using a twin-screw extruder and injection molding, PP/CNTSU composites were synthesized with higher loading. As shown in Fig. 5, the ever increase of thermal enhancement by increasing filler loading can be easily identified. When 10 wt.% of CNTSU was added, thermal conductivity of enhanced composite κ_{CP} reached 0.44 ± 0.01 W/(m·K). Moreover, the higher κ_{CP} from longer CNT growth time thus higher CNT percentage can also be observed when the same 2 wt.% of CNTSU were added. However, the mild κ_{CP} increases from 4 h grown CNTSU compared with that grown for 1 h prompts us to choose 1 h for the following experiments as the sufficient growth time for CNTSU to expand. Composites with CNTSU filler loading higher than 10 wt.% were hindered by the low viscosity to form a uniform dispersion of CNTSU with the direct-mixing.

However, as shown on the fracture surface of above composites (Fig. 4(c) and Fig. S3 in the ESM), by direct-mixing, CNTSUs have not constructed interconnected network, instead CNTSU isolated distributed even for 10 wt.% loading. Moreover, direct-mixing also tended to shrink the outstretching of CNT formed during growth, when compared with the diameter change before and after compounding. Mixing alone prevents an efficient heat conduction network from being achieved. Consequently, low thermal conductive matrix between CNTSU and the high Kapitza resistance at the CNT/matrix interface [28] hindered the heat transfer. To further increase κ_{CP}, presetting a closely interconnected network of CNTSU and increasing the density and uniformity among bulk material become essential.

3.1.2 Percolated network via confined-grown CNTSU

As shown in Fig. 1, the ceramic growth cage prepared by 3D printing combined with the porous AAO walls confined the disorderly expansion of CNTSU during the growth process, forming uniformly compacted CNTSU bulk materials with desired thickness. Based on our previous experiment, reaction gases cannot penetrate through compacted CNTSU thicker than 5 mm. Therefore, we applied the AAO as the confining wall, which can tolerate growth environment and is thin enough for the

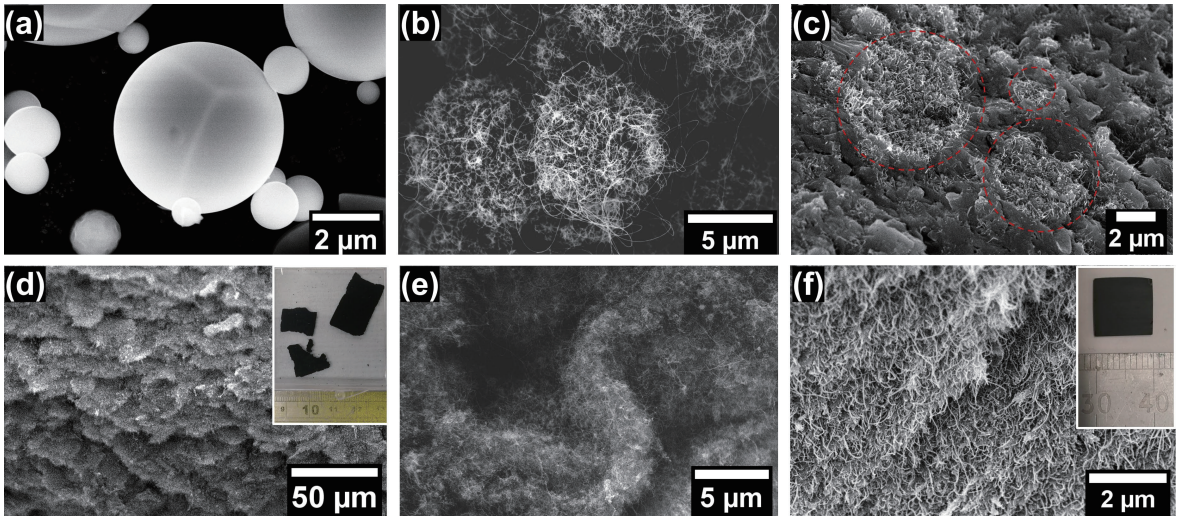

Figure 4 CNTSU used as thermal fillers with free-growth + direct-mixing, and confined-growth + *in-situ* polymerization. (a) The alloy micron cores of aluminium and iron oxides synthesized with a continuous aerosol process. (b) With 1 h of free growth under unlimited expansion, the CNTSU morphology formed with CNT outstretching, expanding the diameter compared with cores. (c) By direct-mixing with a twin-screw extruder, in the final composites, the dispersed CNTSU shrunk on diameter, and even 10 wt.% of loading cannot guarantee the close interconnection between CNTSUs. ((d) and (e)) With custom-made growth cage, the expansion space was confined for the growing CNTSU, forming the CG-CNTSU bulk material (photo inset). During this process, the hollow cores were crushed into oblate spheroids. CNTs among different CG-CNTSUs entangled, forming the hierarchical interconnected 3D network. (f) With CG-CNTSU and *in-situ* polymerization, 21 wt.% high filler loading can be easily realized with preset CNT interconnection maintained within the final composite (photo inset).

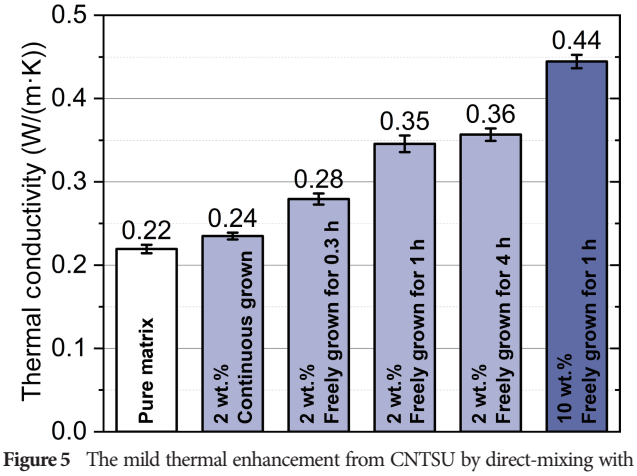

Figure 5 The mild thermal enhancement from CNTSU by direct-mixing with different filler loading and CNTSU growth time.

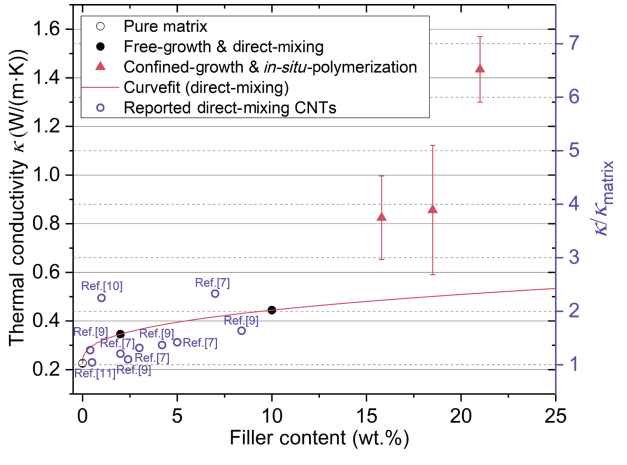

Figure 6 The optimized thermal enhancement from the confined-grown CNTSU and the *in-situ* Polymerization. The κ_{CP} enhancement from the closely interconnected CG-CNTSU is much significant which overtake the prediction of the power-law curve fitting of results from the direct-mixing. The reported CNT thermally enhanced composites were also listed (purple hollow circles) according to their enhancement factor compared with corresponding matrix (compared with right-axis, data details in Table S1 in the ESM).

feeding of reaction gas to supply the growth of CNT through the nanopores on the AAO. As growth started, the expansion of CNT lifted the weight to the maximum allowed space. Then the ever expansion forced CNTs to entangle inward. As the confined-grown CNTSU (CG-CNTSU) squeeze with each other, the original sphere cores cannot be observed within final material anymore, instead the thin shells of hollow cores were easily crushed into oblate spheroid and debris, finally building the closely interconnected high-density CNTSU bulk material (Figs. 4(d) and 4(e)), referred as the CG-CNTSU. CNTs among different CNTSUs are entangled, forming the isotropic and interconnected network. The density of the CG-CNTSU with 1 h growth is ~ 0.20 g/cm^3. As a result of the close interconnections between CNTSUs, the CG-CNTSU bulk material is free-standing (photo inset Fig. 7(d)), which facilitates handling as a preset thermal conduction network.

By using CG-CNTSU as filler and further combined with *in-situ* polymerization, the epoxy/CG-CNTSU composite was synthesized. With the preset highly interconnected heat conduction networks, the CNTSU loading easily surpassed 15 wt.%. More importantly, as shown in Fig. 6, when the filler loading is 15.8 wt.%, κ_{CP} of epoxy/CG-CNTSU composite reached 0.82 ± 0.17 W/(m·K). κ_{CP} further increased to 1.43 ± 0.13 W/(m·K) for 21.0 wt.% of loading, 6.2 times higher than that of the neat epoxy matrix (0.23 ± 0.01 W/(m·K)). The thermal enhancement from the CG-CNTSU and *in-situ* polymerization all surpass the prediction from the power-law curve fitting based on results from the direct-mixing. From the fracture surface of epoxy/CG-CNTSU composites (Fig. 4(e)), *in-situ* polymerization process indeed maintained the dense CNT interconnection formed during growth. Consequently, more pathways are available for phonons when traversing through the composite, giving rise to the thermal enhancement. Above evidence emphasizes the importance of presetting and persisting a closely interconnected heat conduction network.

In addition to thermal conductivity, it is well known that the loading of CNT filler in the composite needs to be high enough to form an effective electricity percolated network. There is no doubt that the highly compacted CG-CNTSU bulk material has formed a percolated network during growth. With 15.8 wt.% and 21.0 wt.% of CG-CNTSU, electricity conductivity of composite

(σ_{CP}) reached 52.2 ± 0.6 and 140.1 ± 4.3 S/m, respectively, more than 6 orders increasing compared with pure epoxy, also much higher than 3.95 ± 0.05 S/m for the direct-mixing composites with 10 wt.% CNTSU powders.

3.2 Composites thermally enhanced by *in-situ* grown aligned hybrid CNT-hBN networks

3.2.1 Thermal enhancement by aligned hBN network with low loading

As we discussed in the introduction section, to construct a 3D closely interconnected heat conduction network with CNT materials, we used the cores as support in building an isotropic network (CNTSU bulk materials) and breaking the loading upper limit. To *in-situ* construct an anisotropic network with preferred heat conduction direction, we used the anisotropic nanomaterials like 2D materials as support to *in-situ* grow CNT.

Although graphene is the best thermal conductive 2D materials (in-plane $\kappa_{//}$ ~ 3000 W/(m·K)), we have not achieved any competitive results with graphene as support materials (brown solid pentagon in Fig. 7). We attempted to use graphene oxide (GO) solution-based method and *in-situ* reduction and CNT growth in building heat conduction network (Fig. S4 in the ESM). We attribute the poor thermal enhancement to the highly defective graphene obtained after reduction GO aerogel and CNT growth. The phonon scattering from defects and crystal boundary might be too serious, hiding the thermal enhancement. Additionally, with current growth parameters, growing CNT from iron catalyst attached on graphene substrate appeared to be inefficient. Only short and curly CNT can be observed. Iron catalysts seemed to deteriorate the rGO surface by etching at high temperature and reduction environment [29, 30].

Therefore, we incorporated hBN as the anisotropic 2D support materials, because of its high temperature resistance, chemical inertness, and outstanding in-plane thermal conductivity ($\kappa_{//}$ ~ 360 W/(m·K)) [31]. However, due to the relative high density of hBN, the micron scale size and the anisotropic κ for individual hBNNF, proper orientation, and connection among hBNNFs become essential to fully utilize their higher in-plane $\kappa_{//}$ instead of out-of-plane $\kappa_{\perp}$ ~ 30 W/(m·K). Furthermore, we found it essential to construct more efficient thermal conduction network with much lower filler loading (< 10 wt.%) rather than commonly used 30 wt.%–60 wt.% [13, 32, 33] which brought in excessive density/weight increase.

As shown in Fig. 2, we utilized directional ice-templating self-assembly and freeze-drying method to organize highly delaminated thin layer hBN. Due to the aligned ice crystal growth arising from the imposed vertical temperature gradient, an aligned hBN network was prepared (Fig. 7(a)). To take advantage of the highly delaminated hBN produced with shear fluid processor, hBN nanoflakes overlapped with each other along the crystal in-plane direction, and finally self-assembled into the hBN nanobelt (hBNNB, Fig. 7(b)). In contrast to other common freeze-drying methods, this directional self-assembly method changes the aerogel as a thermal insulation material composed of randomly distributed hBN. By further concentrating the hBN solution to ~ 3.5 mg/mL, hBNNBs become thicker, wider, and denser in aligned network, finally forming the porous aligned nano-book (Figs. 7(d) and 7(e)).

Owing to the aligned hierarchical organization of hBN, a more efficient thermal conduction network was built with a low filler loading (2 wt.%–7 wt.%). With *in-situ* polymerization, the prepared epoxy/aligned hBNNB composites retained the geometry and uniformity of the hybrid network. As can be observed in Fig. 8 (blue hollow diamond), with 2.5 wt.% and 6.6 wt.% addition of aligned hBN network, κ_{CP} along the desired direction (through thickness) reached 0.29 ± 0.01 and 0.43 ± 0.02 W/(m·K), respectively. As a comparison, by direct-mixing hBN powder within matrix, κ_{CP} are only 0.29 ± 0.01 and 0.38 ± 0.03 W/(m·K) when the loadings are 6.5 wt.% and 12.0 wt.%. In Fig. 8, the difference in trends between the 2 sets of results emphasizes the importance of the delamination process and the well alignment of hBN within hBNNBs. When compared with reported results also based on aligned hBN fillers (purple diamond) but produced with ball-milling [12] or CVD method [16], our results are still superior at similar loading. We attribute this superiority to the higher aspect ratio (AR > 55) of the used hBNNF produced by shear fluid processor [25] than the sonication ones (AR ~ 20, typically 200 nm lateral size, 10 nm thick). This is because with larger lateral size and AR > 40, the nanoflakes tend to align [34] and construct ordered overlapping within nanobelts, the superior in-plane thermal conduction of hBN can thus be better utilized in the conduction pathway. With

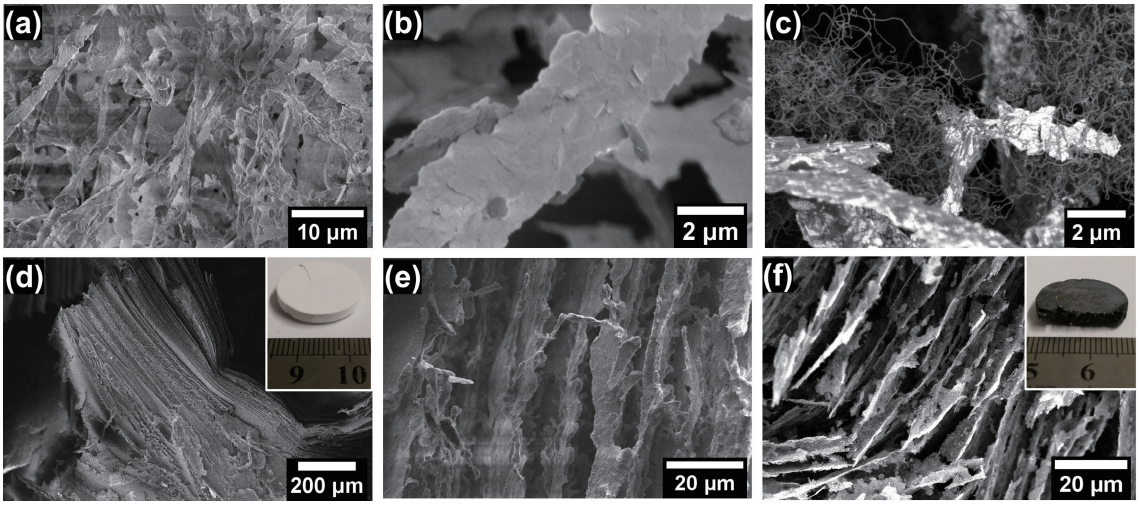

Figure 7 *In-situ* grown aligned CNT-hBN network used as thermal enhancement hybrid fillers. ((a) and (b)) With low concentrated hBN solution (0.44 mg/mL) and directional ice-templating self-assembly method, the hBNNFs self-assembled into aligned hBN nanobelts within the network. ((d) and (e)) By further concentrating the hBN solution to ~ 3.5 mg/mL, the resultant nanobelts become thicker, wider, and denser, finally forming the aligned porous nano-book network (photo inset). With the aligned hBN network as support materials, CNTs were *in-situ* CVD grown from iron catalysts and extended outward from hBN support, interconnecting inter- and intra- hBNNBs through the thickness as illustrated in the fracture surface of both (c) low and (f) high density network (more details in Fig. S5 in the ESM). After the CNT growth, the hybrid network still retained free-standing state as shown in inset photo.

much reduced interface density along conduction direction, phonons scattering in all directions as occurred in random systems can be avoid. Meanwhile, with an improved alignment, the contact area between hBNs is further extended, thus decreasing the contact resistance between hBNs [19]. Therefore, along the axis of hBNNBs, nanoflakes possessing high $\kappa_{//}$ could form an "express highway" to channel the heat. With the enhanced thermal conductivity, the aligned pure hBN composites are indispensable for the application with purposes of both electric insulation and thermal conduction.

3.2.2 *Synergistic effect on the in-situ grown hybrid CNT-hBN aligned network*

With the above aligned hBN network as support material, we constructed the anisotropic network of hybrid CNT-hBN by *in-situ* CNT growth. As shown in Fig. 2, by simply mixing iron oxide as catalysts within hBN solution, the Fe_2O_3 NP can be easily distributed within hBN network after freeze drying. With further *in-situ* CVD growth, CNTs synthesized from iron catalysts outstretched, and interconnected inter and intra hBNNBs within networks of both low and high density (Figs. 7(c) and 7(f)). After the CNT growth, the CNT-hBN network still retained sufficient mechanical strength and free-standing state (photo inset Fig. 7(f)). The typical density for the aligned BN networks with CMC stabilizer mixed is ~ 6 mg/cm^3 after freeze-drying the low concentrated hBN solution, and ~ 33 mg/cm^3 for the further concentrated one. After the *in-situ* CNT growth, the density of the CNT-hBN hybrid networks based on the high density hBN network increased to ~ 37 mg/cm^3. It is worth noting that we have also tried to build CNTSU-hBN hybrid network, however, because of the occupying effect from micron cores, the core-hBN network was too brittle to be free-standing.

By using these hybrid CNT-hBN networks as fillers, the resultant epoxy/CNT-hBN composites demonstrated a higher κ_{CP} than those with similar hBN loading. As shown in Fig. 8 (blue solid diamond), with ~ 5.7 wt.% loading (~ 2.9 wt.% hBN and ~ 2.7 wt.% CNT), κ_{CP} reached 0.61 ± 0.07 W/(m·K), higher than 0.33 ± 0.01 W/(m·K) for the similar hBN loading (~ 3.0 wt.% hBN and ~ 0.3 wt.% Fe_2O_3 NP). The highest κ_{CP} = 0.86 ± 0.14 W/(m·K) came from the ~ 8.5 wt.% hybrid filler among which ~ 6.6 wt.% hBN and ~ 1.4 wt.% CNT, 374% of that for neat matrix. When compared with reports results, similar κ_{CP} (0.85 W/(m·K)) can only reached with vertically aligned hBN–epoxy composites with 20 wt.% hBN loading [15].

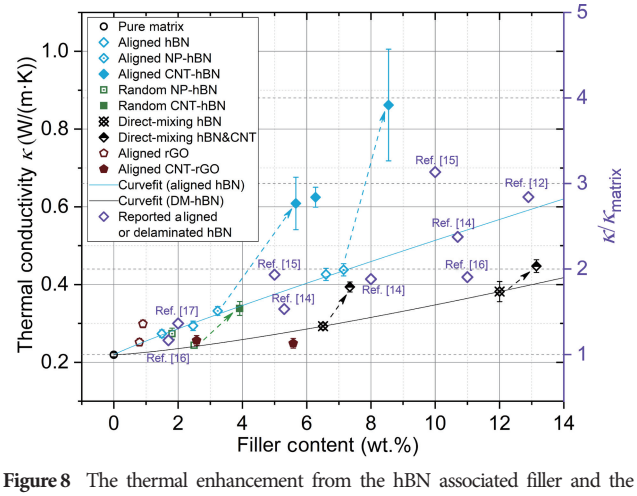

Figure 8 The thermal enhancement from the hBN associated filler and the aligned hybrid CNT-hBN network. Networks of aligned pure hBN and the *in-situ* grown hybrid CNT-hBN acted as superior thermal enhancement fillers than the random distributed hBN networks and control groups with direct-mixing. The synergistic effect from the 1D + 2D nanomaterials can also be identified on the CNT-hBN systems particularly for the *in-situ* grown ones. The reported composites results enhanced by aligned hBN were also listed as purple hollow diamond, which should be compared with the right axis (data details in Table S1 in the ESM). All the other data points were experimental results in this work. Some trials on CNT-graphene network were also presented (more details can be found in Fig. S4 in the ESM).

In recent years, the synergistic effects of simultaneously using 2D (graphene, hBN, etc.) and 1D (CNT, nanofiber, etc.) nanomaterials have been discovered [5, 22, 23, 35, 36]. As shown in Fig. 8 (blue symbols), the κ_{CP} for the hybrid network was higher than the prediction from the curve fitting based on the aligned pure hBN ones. The corresponding thermal enhancement cannot be achieved with only the similar loading of CNTs (2.7 wt.% or 1.4 wt.%). As shown in Fig. 6 (purple circles), according to the reported results [7–11, 37], the thermal enhancement factor from < 3 wt.% loading of CNT was always < 50%, and the increased value < 0.057 W/(m·K) when compared with the epoxy matrix. All these results indicate the formation of a synergistic thermal enhancement effect between 1D CNT and 2D hBN. The thermally bridging hBN 2D nanoflakes with 1D CNTs, extending the conductive 1D–2D hybrid network, increasing the total interfacial area by increasing the filler dimensions, combined with the high cross-plane transmission of phonon modes between CNT and hBN [38], leading to reduction of the thermal interface resistance (R_i) along the network [5]. Additionally, without CNT growth, the epoxy/Fe_2O_3 NP-hBN composites did not show similar synergistic thermal enhancement effect (blue dotted diamond). Instead, κ_{CP} appears to follow the prediction based on the pure hBN, emphasizing the contribution from CNTs to interconnect neighbouring hBN, where the synergistic effect originated.

The synergistic thermal enhancement from CNT-hBN random network can also be observed (green solid square), however, limited by the inefficient conduction through randomly distributed hBN, the thermal enhancement was not remarkable. Moreover, similar synergistic enhancement trend can also be observed from direct-mixing by stirring hBN powders with NC7000 CNT powders within epoxy resin: Both hybrid fillers (half black diamond) show the superior enhancement from the curve fitted prediction based on the direct-mixed solely hBN within a matrix, but the increase in slope is milder compared with that from *in-situ* grown CNT and with similar CNT loading. This should originate from the nonuniform dispersion of the hybrid fillers and the curling up of CNTs by direct-mixing [39]. The high contact resistance between fillers was also generated by tiny contact area and weak interaction between hBN and CNT by direct-mixing [32]. Therefore, both *in-situ* constructing highly interconnected and uniform 1D + 2D hybrid network and aligned organization of fillers seem to be essential in realizing an efficient synergistic thermal enhancement effect.

Besides the above successive discussion on CNT-cores and CNT-hBN hybrid networks as the isotropic and anisotropic fillers respectively, some similarities can be found between them. Because both CNT-cores and CNT-hBN hybrid networks were constructed by casting in a mold, we can expect to achieve thermal enhanced composites with irregular shapes by *in-situ* polymerizing the *in-situ* grown irregular shaped network with preset thermal conduction performance. For hybrid CNT-cores network, since the CG-CNTSU bulk material is derived from the growth and expansion of CNT, the shape of the bulk material can cast the shape of cage space (shape transfer [40]). While for hybrid CNT-hBN network, the freeze-casting and freeze-drying process guaranteed the network to cast the shape of mold. Combined with *in-situ* polymerization to persist the network after compounding, the advantage of irregular manufacturing of injection molding by direct-mixing can still be retained while the troublesome dispersing of filler within matrix can be avoided.

4 Conclusions

To enhance the thermal performance of polymer composites with nano-structured materials, such as CNTs, we found the importance of establishing a fully percolated CNT heat conduction 3D network and maintaining this network throughout the polymerization process. To further establish a desired isotropic and preferred directional heat conduction, we incorporated micron spherical cores and hBN nanoflakes respectively as support materials to construct the hybrid CNT-support 3D networks with *in-situ* CNT growth. More specifically, with cores as the support, we developed an *in-situ* confined-growth technique for CNT-core (CNTSU) materials to construct an isotropic network as efficient phonon transport pathway, which easily surpassed 15 wt.% loading limitation and solved the nonuniform filler dispersion and agglomeration problem for traditional direct-mixing method. When the loading further increased to 21.0 wt.%, the thermal conductivity of composites reached 1.43 ± 0.13 W/(m·K). Alternatively, with high aspect ratio hBN as the support, we constructed a CNT-hBN hybrid aligned network by *in-situ* CNT growth. With relative low loading (~ 8.5 wt.%) of hybrid filler to avoid excessive density increase from hBN, the composites possess thermal conductivity up to 0.86 ± 0.14 W/(m·K), which is 374% of that for neat polymer matrix. The synergistic thermal enhancement from 1D + 2D hybrid materials becomes more distinct due to the uniform distribution of expanded CNTs within hybrid network. These *in-situ* constructed 3D networks show better performance compared with control samples fabricated by direct-mixing. This study paves the way for thermally conductive polymer composites used as thermal interface materials for next-generation electronic packaging and 3D integration circuits, particularly when both directional thermal conduction and complex composite geometry are simultaneously required.

Acknowledgements

This work was partially supported by the National Key R&D Program of China (Nos. 2018YFA0208402 and 2020YFA0714700), the National Natural Science Foundation of China (Nos. 52172060, 51820105002, 11634014, and 51372269), Magna International, and EPSRC project "Advanced Nanotube Application and Manufacturing (ANAM) Initiative" (No. EP/M015211/1). The authors especially thank Mr. David Paul, Ms. Mingzhao Wang, Ms. Rulan Qiao, and Dr. Sarah Stevenson, for their kind support and useful discussion.

Funding note: Open access funding provided by JISC.

Electronic Supplementary Material: Supplementary material (further details of 3D printed cage component, the *in-situ* polymerization with vacuum bag method, thermal conductivity measurement setup and its mechanism, evolution of CNTSU and its composites with growth time, graphene-based hybrid fillers, CNT-hBN hybrid structure, and table for all the cited data points in figures) is available in the online version of this article at https://doi.org/10.1007/s12274-023-6209-6.

References

[1] Pernot, G.; Stoffel, M.; Savic, I.; Pezzoli, F.; Chen, P.; Savelli, G.; Jacquot, A.; Schumann, J.; Denker, U.; Mönch, I. et al. Precise control of thermal conductivity at the nanoscale through individual phonon-scattering barriers. *Nat. Mater.* **2010**, *9*, 491–495.

[2] Li, R.; Yang, X.; Li, J.; Shen, Y.; Zhang, L.; Lu, R.; Wang, C.; Zheng, X.; Chen, H.; Zhang, T. Review on polymer composites with high thermal conductivity and low dielectric properties for electronic packaging. *Mater. Today Phys.* **2022**, *22*, 100594.

[3] Song, Y. W.; Perez, C.; Esteves, G.; Lundh, J. S.; Saltonstall, C. B.; Beechem, T. E.; Yang, J. I.; Ferri, K.; Brown, J. E.; Tang, Z. C. et al. Thermal conductivity of aluminum scandium nitride for 5G mobile applications and beyond. *ACS Appl. Mater. Interfaces* **2021**, *13*, 19031–19041.

[4] Moore, A. L.; Shi, L. Emerging challenges and materials for thermal management of electronics. *Mater. Today* **2014**, *17*, 163–174.

[5] Yu, A. P.; Ramesh, P.; Sun, X. B.; Bekyarova, E.; Itkis, M. E.; Haddon, R. C. Enhanced thermal conductivity in a hybrid graphite nanoplatelet-carbon nanotube filler for epoxy composites. *Adv. Mater.* **2008**, *20*, 4740–4744.

[6] Liang, Q. Z.; Moon, K. S.; Jiang, H. J.; Wong, C. P. Thermal conductivity enhancement of epoxy composites by interfacial covalent bonding for underfill and thermal interfacial materials in Cu/Low-K application. *IEEE Trans. Compon. Packag. Manufact. Technol.* **2012**, *2*, 1571–1579.

[7] Du, F. M.; Guthy, C.; Kashiwagi, T.; Fischer, J. E.; Winey, K. I. An infiltration method for preparing single-wall nanotube/epoxy composites with improved thermal conductivity. *J. Polym. Sci. Part B: Polym. Phys.* **2006**, *44*, 1513–1519.

[8] Marconnet, A. M.; Yamamoto, N.; Panzer, M. A.; Wardle, B. L.; Goodson, K. E. Thermal conduction in aligned carbon nanotube-polymer nanocomposites with high packing density. *ACS Nano* **2011**, *5*, 4818–4825.

[9] Bryning, M. B.; Milkie, D. E.; Islam, M. F.; Kikkawa, J. M.; Yodh, A. G. Thermal conductivity and interfacial resistance in single-wall carbon nanotube epoxy composites. *Appl. Phys. Lett.* **2005**, *87*, 161909.

[10] Biercuk, M. J.; Llaguno, M. C.; Radosavljevic, M.; Hyun, J. K.; Johnson, A. T.; Fischer, J. E. Carbon nanotube composites for thermal management. *Appl. Phys. Lett.* **2002**, *80*, 2767–2769.

[11] Gojny, F. H.; Wichmann, M. H. G.; Fiedler, B.; Kinloch, I. A.; Bauhofer, W.; Windle, A. H.; Schulte, K. Evaluation and identification of electrical and thermal conduction mechanisms in carbon nanotube/epoxy composites. *Polymer* **2006**, *47*, 2036–2045.

[12] Hu, J. T.; Huang, Y.; Yao, Y. M.; Pan, G. R.; Sun, J. J.; Zeng, X. L.; Sun, R.; Xu, J. B.; Song, B.; Wong, C. P. Polymer composite with improved thermal conductivity by constructing a hierarchically ordered three-dimensional interconnected network of BN. *ACS Appl. Mater. Interfaces* **2017**, *9*, 13544–13553.

[13] He, H. Y.; Peng, W. X.; Liu, J. B.; Chan, X. Y.; Liu, S. K.; Lu, L.; Le Ferrand, H. Microstructured BN composites with internally designed high thermal conductivity paths for 3D electronic packaging. *Adv. Mater.* **2022**, *34*, 2205120.

[14] Han, W. F.; Bai, Y. F.; Liu, S. C.; Ge, C. H.; Wang, L. X.; Ma, Z. Y.; Yang, Y. X.; Zhang, X. D. Enhanced thermal conductivity of commercial polystyrene filled with core-shell structured BN@PS. *Compos. Part A: Appl. Sci. Manuf.* **2017**, *102*, 218–227.

[15] Lin, Z. Y.; Liu, Y.; Raghavan, S.; Moon, K. S.; Sitaraman, S. K.; Wong, C. P. Magnetic alignment of hexagonal boron nitride platelets

in polymer matrix: Toward high performance anisotropic polymer composites for electronic encapsulation. *ACS Appl. Mater. Interfaces* **2013**, *5*, 7633–7640.

[16] Wang, X. B.; Weng, Q. H.; Wang, X.; Li, X.; Zhang, J.; Liu, F.; Jiang, X. F.; Guo, H. X.; Xu, N. S.; Golberg, D. et al. Biomass-directed synthesis of 20 g high-quality boron nitride nanosheets for thermoconductive polymeric composites. *ACS Nano* **2014**, *8*, 9081–9088.

[17] Morishita, T.; Okamoto, H. Facile exfoliation and noncovalent superacid functionalization of boron nitride nanosheets and their use for highly thermally conductive and electrically insulating polymer nanocomposites. *ACS Appl. Mater. Interfaces* **2016**, *8*, 27064–27073.

[18] Kinloch, I. A.; Suhr, J.; Lou, J.; Young, R. J.; Ajayan, P. M. Composites with carbon nanotubes and graphene: An outlook. *Science* **2018**, *362*, 547–553.

[19] Shenogina, N.; Shenogin, S.; Xue, L.; Keblinski, P. On the lack of thermal percolation in carbon nanotube composites. *Appl. Phys. Lett.* **2005**, *87*, 133106.

[20] Zhang, X.; Tan, W.; Smail, F.; De Volder, M.; Fleck, N.; Boies, A. High-fidelity characterization on anisotropic thermal conductivity of carbon nanotube sheets and on their effects of thermal enhancement of nanocomposites. *Nanotechnology* **2018**, *29*, 365708.

[21] Zhan, H. F.; Nie, Y. H.; Chen, Y. N.; Bell, J. M.; Gu, Y. T. Thermal transport in 3D nanostructures. *Adv. Funct. Mater.* **2020**, *30*, 1903841.

[22] Zhong, S. L.; Zhou, Z. Y.; Zhang, K.; Shi, Y. D.; Chen, Y. F.; Chen, X. D.; Zeng, J. B.; Wang, M. Formation of thermally conductive networks in isotactic polypropylene/hexagonal boron nitride composites via "Bridge Effect" of multi-wall carbon nanotubes and graphene nanoplatelets. *RSC Adv.* **2016**, *6*, 98571–98580.

[23] Im, H.; Kim, J. Thermal conductivity of a graphene oxide-carbon nanotube hybrid/epoxy composite. *Carbon* **2012**, *50*, 5429–5440.

[24] de La Verpilliere, J.; Jessl, S.; Saeed, K.; Ducati, C.; De Volder, M.; Boies, A. Continuous flow chemical vapour deposition of carbon nanotube sea urchins. *Nanoscale* **2018**, *10*, 7780–7791.

[25] Carey, T.; Cacovich, S.; Divitini, G.; Ren, J. S.; Mansouri, A.; Kim, J. M.; Wang, C. X.; Ducati, C.; Sordan, R.; Torrisi, F. Fully inkjet-printed two-dimensional material field-effect heterojunctions for wearable and textile electronics. *Nat. Commun.* **2017**, *8*, 1202.

[26] Zhang, Y. G.; Zhu, Y. J.; Chen, F.; Sun, T. W. Biocompatible, ultralight, strong hydroxyapatite networks based on hydroxyapatite microtubes with excellent permeability and ultralow thermal conductivity. *ACS Appl. Mater. Interfaces* **2017**, *9*, 7918–7928.

[27] Bozlar, M.; He, D. L.; Bai, J. B.; Chalopin, Y.; Mingo, N.; Volz, S. Carbon nanotube microarchitectures for enhanced thermal conduction at ultralow mass fraction in polymer composites. *Adv. Mater.* **2010**, *22*, 1654–1658.

[28] Nan, C. W.; Birringer, R.; Clarke, D. R.; Gleiter, H. Effective thermal conductivity of particulate composites with interfacial thermal resistance. *J. Appl. Phys.* **1997**, *81*, 6692–6699.

[29] Datta, S. S.; Strachan, D. R.; Khamis, S. M.; Johnson, A. T. C. Crystallographic etching of few-layer graphene. *Nano Lett.* **2008**, *8*, 1912–1915.

[30] Lukas, M.; Meded, V.; Vijayaraghavan, A.; Song, L.; Ajayan, P. M.; Fink, K.; Wenzel, W.; Krupke, R. Catalytic subsurface etching of nanoscale channels in graphite. *Nat. Commun.* **2013**, *4*, 1379.

[31] Jo, I.; Pettes, M. T.; Kim, J.; Watanabe, K.; Taniguchi, T.; Yao, Z.; Shi, L. Thermal conductivity and phonon transport in suspended few-layer hexagonal boron nitride. *Nano Lett.* **2013**, *13*, 550–554.

[32] Pak, S. Y.; Kim, H. M.; Kim, S. Y.; Youn, J. R. Synergistic improvement of thermal conductivity of thermoplastic composites with mixed boron nitride and multi-walled carbon nanotube fillers. *Carbon* **2012**, *50*, 4830–4838.

[33] Sato, K.; Horibe, H.; Shirai, T.; Hotta, Y.; Nakano, H.; Nagai, H.; Mitsuishi, K.; Watari, K. Thermally conductive composite films of hexagonal boron nitride and polyimide with affinity-enhanced interfaces. *J. Mater. Chem.* **2010**, *20*, 2749–2752.

[34] Kelly, A. G.; O'Suilleabhain, D.; Gabbett, C.; Coleman, J. N. The electrical conductivity of solution-processed nanosheet networks. *Nat. Rev. Mater.* **2022**, *7*, 217–234.

[35] Che, J. J.; Jing, M. F.; Liu, D. Y.; Wang, K.; Fu, Q. Largely enhanced thermal conductivity of HDPE/boron nitride/carbon nanotubes ternary composites via filler network-network synergy and orientation. *Compos. Part A: Appl. Sci. Manuf.* **2018**, *112*, 32–39.

[36] Li, W. K.; Dichiara, A.; Bai, J. B. Carbon nanotube-graphene nanoplatelet hybrids as high-performance multifunctional reinforcements in epoxy composites. *Compos. Sci. Technol.* **2013**, *74*, 221–227.

[37] Bonnet, P.; Sireude, D.; Garnier, B.; Chauvet, O. Thermal properties and percolation in carbon nanotube-polymer composites. *Appl. Phys. Lett.* **2007**, *91*, 201910.

[38] Liu, Y.; Ong, Z. Y.; Wu, J.; Zhao, Y. S.; Watanabe, K.; Taniguchi, T.; Chi, D. Z.; Zhang, G.; Thong, J. T. L.; Qiu, C. W. et al. Thermal conductance of the 2D MoS_2/*h*-BN and graphene/*h*-BN interfaces. *Sci. Rep.* **2017**, *7*, 43886.

[39] Guthy, C.; Du, F. M.; Brand, S.; Winey, K. I.; Fischer, J. E. Thermal conductivity of single-walled carbon nanotube/PMMA nanocomposites. *J. Heat Transfer* **2007**, *129*, 1096–1099.

[40] Hart, A. J.; Slocum, A. H. Force output, control of film structure, and microscale shape transfer by carbon nanotube growth under mechanical pressure. *Nano Lett.* **2006**, *6*, 1254–1260.